ARMY RESEARCH LABORATORY

Real-Time Dynamic Impact Strain Deformation Measurements of Transparent Poly(urethane urea) Materials

by Jian H. Yu and Alex J. Hsieh

NOTICES

Disclaimers

The findings in this report are not to be construed as an official Department of the Army position unless so designated by other authorized documents.

Citation of manufacturer's or trade names does not constitute an official endorsement or approval of the use thereof.

Destroy this report when it is no longer needed. Do not return it to the originator.

Army Research Laboratory

Aberdeen Proving Ground, MD 21005

ARL-TR-5355   **September 2010**

Real-Time Dynamic Impact Strain Deformation Measurements of Transparent Poly(urethane urea) Materials

Jian H. Yu and Alex J. Hsieh
Weapons and Materials Research Directorate, ARL

REPORT DOCUMENTATION PAGE			*Form Approved* OMB No. 0704-0188

Public reporting burden for this collection of information is estimated to average 1 hour per response, including the time for reviewing instructions, searching existing data sources, gathering and maintaining the data needed, and completing and reviewing the collection information. Send comments regarding this burden estimate or any other aspect of this collection of information, including suggestions for reducing the burden, to Department of Defense, Washington Headquarters Services, Directorate for Information Operations and Reports (0704-0188), 1215 Jefferson Davis Highway, Suite 1204, Arlington, VA 22202-4302. Respondents should be aware that notwithstanding any other provision of law, no person shall be subject to any penalty for failing to comply with a collection of information if it does not display a currently valid OMB control number.
PLEASE DO NOT RETURN YOUR FORM TO THE ABOVE ADDRESS.

1. REPORT DATE *(DD-MM-YYYY)*	2. REPORT TYPE	3. DATES COVERED (From - To)
September 2010	Final	

4. TITLE AND SUBTITLE	5a. CONTRACT NUMBER
Real-Time Dynamic Impact Strain Deformation Measurements of Transparent Poly(urethane urea) Materials	
	5b. GRANT NUMBER
	5c. PROGRAM ELEMENT NUMBER

6. AUTHOR(S)	5d. PROJECT NUMBER
Jian H. Yu and Alex J. Hsieh	
	5e. TASK NUMBER
	5f. WORK UNIT NUMBER

7. PERFORMING ORGANIZATION NAME(S) AND ADDRESS(ES)	8. PERFORMING ORGANIZATION REPORT NUMBER
U.S. Army Research Laboratory ATTN: RDRL-WMM-B Aberdeen Proving Ground, MD 21005	ARL-TR-5355

9. SPONSORING/MONITORING AGENCY NAME(S) AND ADDRESS(ES)	10. SPONSOR/MONITOR'S ACRONYM(S)
	11. SPONSOR/MONITOR'S REPORT NUMBER(S)

12. DISTRIBUTION/AVAILABILITY STATEMENT
Approved for public release; distribution unlimited.

13. SUPPLEMENTARY NOTES

14. ABSTRACT

Transparent poly(urethane urea) (PUU) materials with tunable microstructures offer an avenue to enable material designs with desired dynamic mechanical deformation properties. This report presents recent experimental findings of select model PUU materials upon ballistic impact testing. Tailoring the microstructure appears to be a dominant factor in altering the rate-dependent mechanical deformation behavior, while promoting phase mixing gives rise to dynamic strain hardening, which is validated by the real-time 3D strain evolution measurements via digital photogrammetry. These efforts are a part of an ongoing research project focused on investigating the microstructure-property relationships of PUUs, in an attempt to elucidate the molecular mechanisms key to simultaneous improvements in both physical and mechanical properties.

15. SUBJECT TERMS
Poly(urethane urea); impact, dynamic strain hardening; photogrammetry

16. SECURITY CLASSIFICATION OF:			17. LIMITATION OF ABSTRACT	18. NUMBER OF PAGES	19a. NAME OF RESPONSIBLE PERSON Jian H. Yu
a. REPORT	b. ABSTRACT	c. THIS PAGE	UU	24	19b. TELEPHONE NUMBER *(Include area code)*
Unclassified	Unclassified	Unclassified			(410) 306-0698

Standard Form 298 (Rev. 8/98)
Prescribed by ANSI Std. Z39.18

Contents

List of Figures

List of Tables

Acknowledgments

INTENTIONALLY LEFT BLANK.

1. Introduction

Hyper-elastic materials are currently used in a wide variety of Army and DoD platforms, which include chem/bio shields or lenses, structure adhesives, foams, composite structures, and films for structural retrofit. Transparent poly(urethane urea) (PUU) materials possess good chemical barrier properties and have been evaluated to replace polycarbonate in eye-protective and face-shield applications. The chemistries of PUU, like polyurethane, are versatile; PUUs with tunable microstructures have shown the potential to enable material designs with simultaneous enhancements in both physical and mechanical properties (*1*).

The thermodynamic incompatibility of the soft segments (SS) and hard segments (HS) leads to a phase-separated microstructure in PUUs. Increasing the HS content typically increases the stiffness and flow stress levels, as well. On the other hand, by simply altering the molecular weight (MW) of the SS—for example, in the case of poly(tetramethylene oxide) (PTMO)—from 2,000 (2K) to 1,000 (1K) g/mol, PUUs have shown enhanced phase mixing; the glass transition of the SS shifts towards higher temperatures (*1, 2*). As a result, PUU materials with PTMO of 1K MW display greater rate-dependent mechanical deformation behavior than the corresponding PUU materials with 2K MW PTMO (*1, 2*). Additionally, drastic improvement in permeation resistance against chloroethyl ethyl sulfide, which is commonly chosen as a stimulant for the chemical warfare blister agent, sulfur mustard gas HD, was observed (*1*). These include significantly longer breakthrough time and slower steady-state flux in the 1K PUU materials over the corresponding 2K PUUs having similar HS contents (*1*).

We have observed that increasing the Shore A or D hardness values improved the ballistic impact performance of polyurethane or PUU materials. In this work, the ballistic impact performance of select model PUU materials is evaluated. Further, the composition dependence of the mode of deformation upon ballistic impact is investigated to determine whether the extent of tensile strain to failure or greater dynamic strain hardening of PUUs is favored to facilitate improved impact performance. This study uses photogrammetry, a digital imaging correlation technique, to determine the local strain evolution of select PUU materials during the ballistic impact testing. This technique permits real-time visualization of a deformation event, as well as the determination of geometric properties (e.g., the displacement and strain history) by tracking the minute changes on the area of interest. With the advancement in digital imaging technology, there has been a strong effort to develop a robust photogrammetric technique for real-time mechanical deformation analysis (*3–5*) in a broad range of materials characterization including biomechanics (*6, 7*), structural engineering (*8, 9*), and ballistics (*10–13*). Results from the local strain deformation measurements will also be used for correlation with the corresponding viscoelastic relaxation data.

2. Experimental

2.1 Materials

In this work, a set of model PUU materials with varying molar ratio of PTMO, 4,4'-dicyclohexylmethane diisocyanate (HMDI) and diethyltoulenediamine (DETA), and molecular weight (MW) of PTMO (650, 1000 and 2000 g/mol) are chosen. In the sample nomenclature (table 1), the numerals "x-y-z" refer to the molar ratio of diisocyanate : diamine chain extender : PTMO, and the succeeding "650," "1K," or "2K" refers to the MW of PTMO as 650, 1K, or 2K g/mol, respectively. Table 1 lists the composition, including the HS% and the SS MW of PUUs studied in this work. The HS% was calculated using an approach based on the urea content, as described by O'Sickey et al. in equation 1 (14):

$$\%HS = \frac{100\ (R\text{-}1)(M_{di} + M_{da})}{(M_g + R(M_{di}) + (R-1)(M_{da}))},$$

(1)

where R is the molar ratio of the diisocyanate to PTMO, and M_{di}, M_{da}, and M_g are the number average MW of the diisocyanate, diamine, and PTMO, respectively. Equation 1 accounts only for the portion of diisocyanate that reacts with diamine and, hence, it primarily represents the material residing in the hard domains (14). The experimental results described in the following sections will be examined in correlation with the HS% values noted here. The Shore hardness was measured according to ASTM-D2240 (15).

Table 1. Compositions, hard segment contents, and Shore A and D hardness values of select PUUs.

Sample ID	Molar ratio HMDI: DETA: PTMO	MW (gm/mol) PTMO	HS (%)	Hardness	
				Shore A	Shore D
PUU 2-1-1 2K	2:1:1		16	81	32
PUU 3-2-1 2K	3:2:1		28	96	54
PUU 4-3-1 2K	4:3:1	2000	37	99	62
PUU 2-1-1 1K	2:1:1		26	96	52
PUU 3-2-1 1K	3:2:1		41	99	70
PUU 4-3-1 1K	4:3:1	1000	51	100	79
PUU 2-1-1 650	2:1:1	650	33	99	69
PUU 5-4-1 2K	5:4:1	2000	44	99	70

2.2 Small Angle X-ray Scattering (SAXS)

SAXS measurements were carried out with a customized 3 m pinhole collimated SAXS camera. A Rigaku Ultrax18 rotating anode with a copper target was operated at 40 kV/60 mA to generate X-rays with $\lambda = 1.5418$ Å. Two-dimensional (2D) data sets were collected using a Molecular

Metrology 2D multi-wire area detector placed ~65 cm from the sample. SAXS data of PUU 2-1-1 2K and PUU 2-1-1 1K were highlighted to show the influence of SS MW on microstructure.

2.3   Dynamic Mechanical Analysis (DMA)

DMA testing was carried out using a TA Instruments Q800 DMA in an oscillatory tension mode. Film samples of 2 mm in width and 1 mm thick were used, and the grip-to-grip distance was about 10 mm. Measurements were conducted at a frequency of 1 Hz for a temperature range of −100 to 150 °C at a heating rate of 1 °C/min.

2.4   Ballistic Impact

Ballistic impacts measurements were carried out with either a 17-grain (1.1-g), 0.22-caliber fragment simulating projectile (FSP) or a 5.56 mm diameter stainless steel sphere (Type 302, 0.69 g). The gas gun was pressurized at different pressures with helium to propel the projectile to reach select impact velocities. The speed of the projectile was tracked with Doppler radar (BR-3502, Infinition Inc.). The PUU target (20 cm × 15 cm × 0.3 cm) was sandwiched in a target frame with a circular opening that was 7.62 cm in diameter. The targets were spray-painted with a random pattern of white and black dots (figure 1). The dot size that appeared on the digital image was about 8 pixels in diameter.
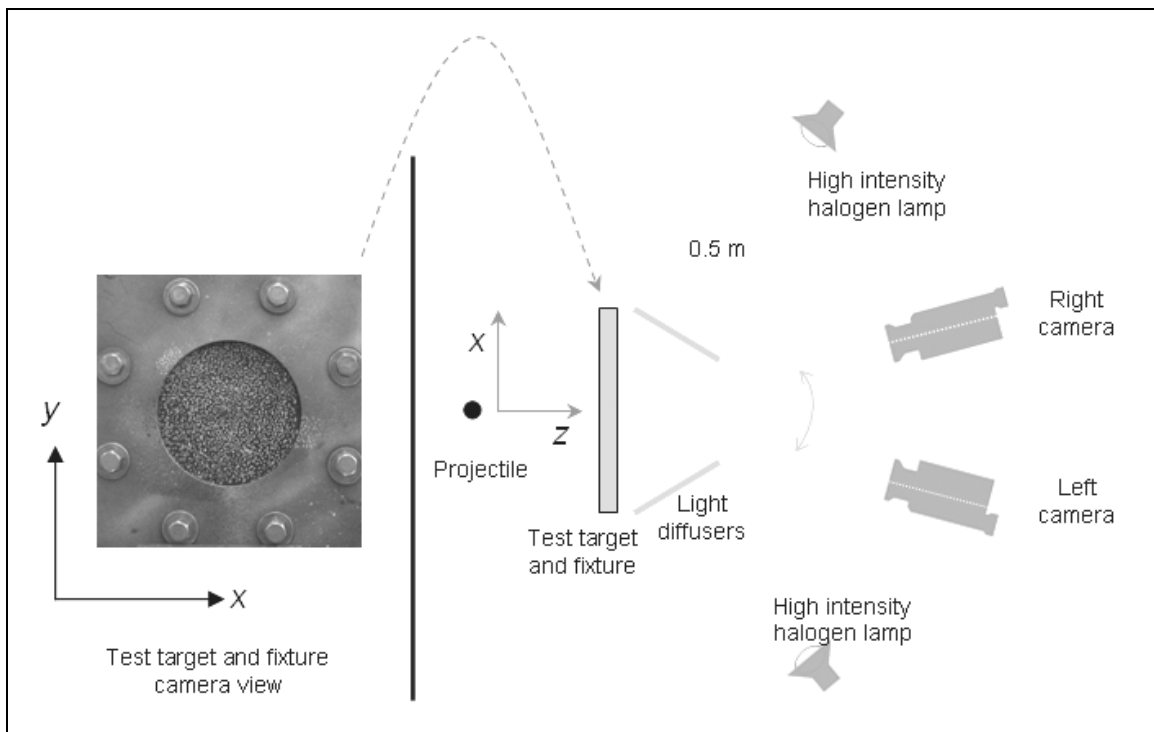

Figure 1. Impact experiment setup.

Two high-speed cameras (Photron SA1, Photron USA, Inc.) were used to generate stereo image pairs of the impact area. The two cameras were placed behind the target fixture. Details of the

camera set-up and images collection can be found in (*13*). The stereo images were analyzed using a commercially available photogrammetric software program, ARAMIS (GOM GmbH, Germany, distributed by Trilion Quality Systems in the USA). The cameras were calibrated with a series of standard dot images (*13, 17*). ARAMIS has a built-in algorithm for calculating the displacement. Details of the data analysis, including the determination of the displacement measurement sensitivity and the strain calculation sensitivity, can be found in (*12, 17*). The ARAMIS software allows for calculation of displacement history in the transverse direction (ε_{yy}), as well as the corresponding shear component (ε_{xy}). In this work, the values of von Mises strain calculated based upon the assumption of a plane-stress loading condition (*18*) were also used in the strain history plots for the purpose of comparing the overall local strain deformation.

3. Results and Discussion

3.1   Extent of Phase Mixing

As previously mentioned, altering the SS MW from 2K to 1K g/mol resulted in greater phase mixing in the 1K PUU materials than in the 2K PUU materials. The extent of phase mixing is characterized by comparing the scattering intensity profiles obtained from SAXS and the viscoelastic relaxation from DMA.

Figure 2 is a highlight comparing the scattering intensities for PUU 2-1-1 2K and PUU 2-1-1 1K. PUU 2-1-1 2K exhibits a well-defined scattering peak, suggesting the presence of isolated HS domains, as is typically observed in microphase-separated PUUs. The scattering characteristics differ when the SS MW is varied. As expected, longer SS (2K MW), while keeping the same molar ratio, contributes to a larger inter-domain spacing (correspondingly, a lower q value). PUU 2-1-1 1K nevertheless exhibits a significant decrease in scattering intensity and a much broader scattering peak, suggesting greater phase mixing.
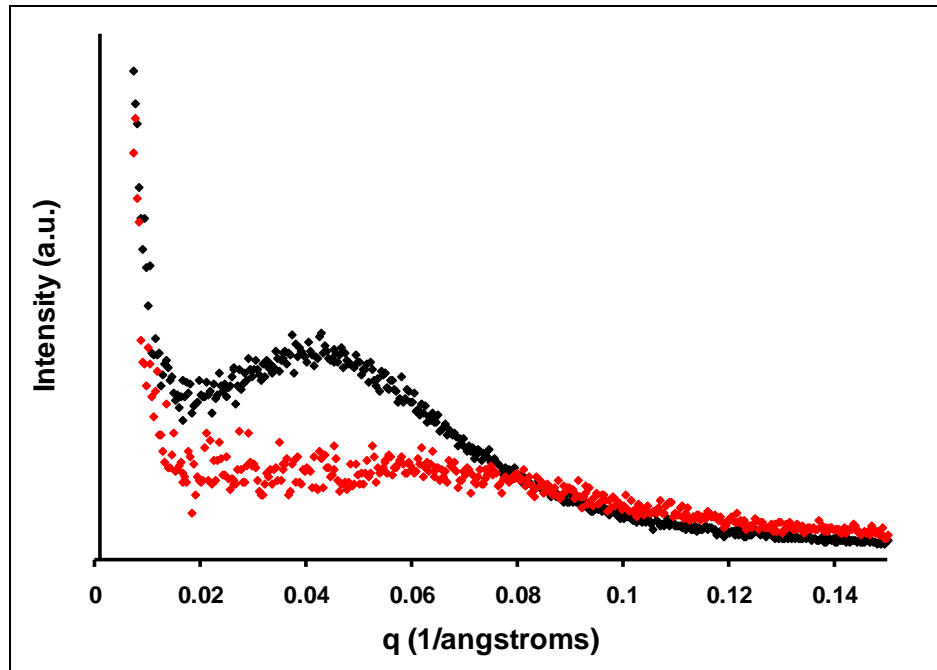
Figure 2. SAXS data for PUU 2-1-1 2K (black) and PUU 2-1-1 1K (red).

Variation in the SS MW also has a large effect on the SS glass transition temperature (T_g). A shift of the SS T_g ~18 °C towards a higher temperature in PUU 2-1-1 1K than in PUU 2-1-1 2K indicates that PUU 2-1-1 1K exhibits greater phase mixing. This is consistent with the SAXS data. Also, the nature of the tanδ peaks is vastly different between these two PUU materials. PUU 2-1-1 2K exhibits a very distinct and intense peak at −64 ℃, along with a weaker shoulder at 21 ℃, as shown in Figure 3. The more intense and dominant peak relates to the relaxation of the SS rich phase, and the weaker shoulder presumably relates to SS in the inter-phase regions (*1, 2, 16*). PUU 2-1-1 1K, on the other hand, displays a single broad tanδ peak, which appears to be a result of the merging of the two SS relaxation peaks that is observed in PUU 2-1-1 2K (*1, 2*).
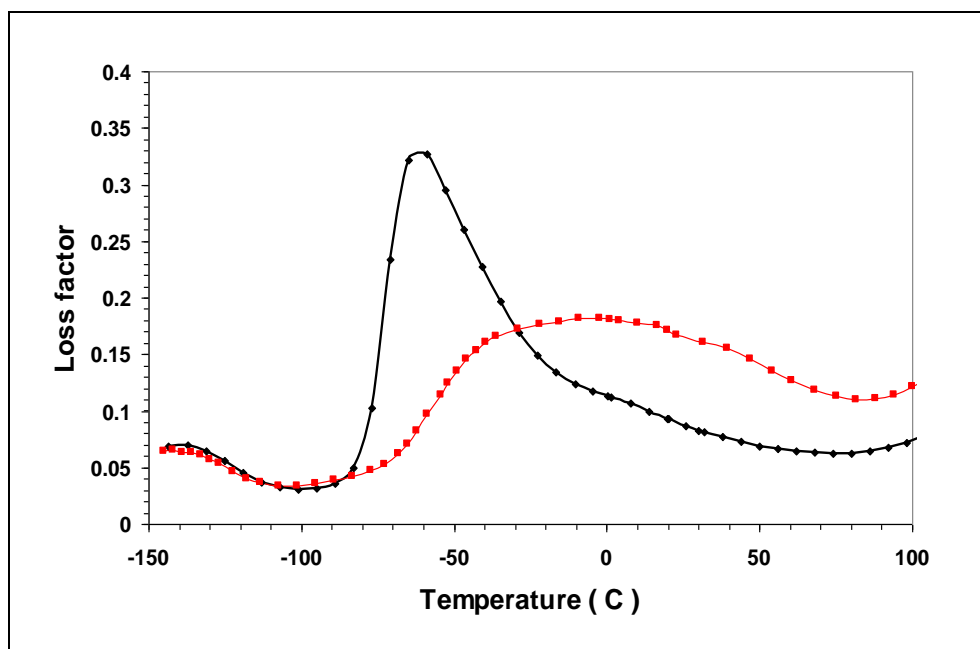
Figure 3. Plots of tanδ (loss factor) as a function of temperature obtained via DMA for PUU 2-1-1 2K (black) and PUU 2-1-1 1K (red).

3.2 Dynamic Impact Deformation

Earlier results showed that increasing the hard segment content in the 2K PUUs conversely increased hardness, resulting in improved ballistic impact performance in PUU 4-3-1 2K (37 HS%) over the PUU 2-1-1 2K (16 HS%). Figure 4a is a photograph that shows a typical ductile mode of failure observed in PUUs after impact against a 0.22-cal FSP. It is noted that the size of the penetration-induced opening was much smaller than the diameter of the projectile, which makes it plausible that the hyper-elastic tensile strength and elongation characteristics may play an important role during the impact deformation. This is significantly different from a typical plug failure seen in polycarbonate.

In this work, a new set of model PUUs consisting of a broad range of compositions is evaluated to determine the influence of SS MW on the impact performance of PUUs. It is noted that PUUs with 1K MW SS generally have higher HS% than the corresponding 2K PUUs having the same stoichiometric molar ratio of diisocyanate : diamine chain extender : PTMO. For example, the HS% of PUU 2-1-1 1K and PUU 2-1-1 2K are 26% and 16%, respectively. In the 1K series, the stiffness and harness can further increase drastically by increasing the HS%; PUU 4-3-1 1K is significantly stiffer than PUU 2-1-1 1K. While PUU 2-1-1 1K exhibits a ductile mode of deformation, PUU 4-3-1 1K displays a change in the failure mode from a ductile to a brittle failure, as shown in figure 4b. The composition dependence of the impact response appears to correlate well with the corresponding quasi-static tensile deformation; PUU 4-3-1 1K exhibits the highest modulus and flow stress values but the lowest strain to failure among the select model PUUs. Results from an earlier work indicated that the strain to failure under tensile testing

decreased as the HS content increased, suggesting an increasing continuity, percolation, or networked hard domains structure as the HS content is increased (*1*).
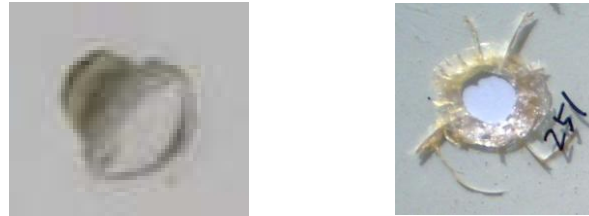

Figure 4. Mode of deformation of PUU materials after
ballistic impact against a 0.22-caliber FSP;
(a) ductile deformation, and (b) brittle failure.

The question is whether a greater strain-to-failure or dynamic strain hardening is more desired in terms of the overall impact performance for these hyper-elastic PUU materials. In this work, a digital imaging correlation technique, which allows for real-time visualization of an impact deformation event, is utilized to determine the local strain evolution of select PUU materials. Figure 5 shows the time histories of the deformed surfaces of the targets, including PUU2-1-1 2K, PUU 3-2-1 2K, PUU 4-3-1 2K, and PUU 3-2-1 1K, which were impacted by a steel sphere at about 106 m/s. The von Mises strain contours are overlaid over the deformed surface. The full-field displacement profiles reveal that PUU exhibits global bending deformation, and additionally the composition dependence of the extent of dynamic deformation strain among these model PUUs.
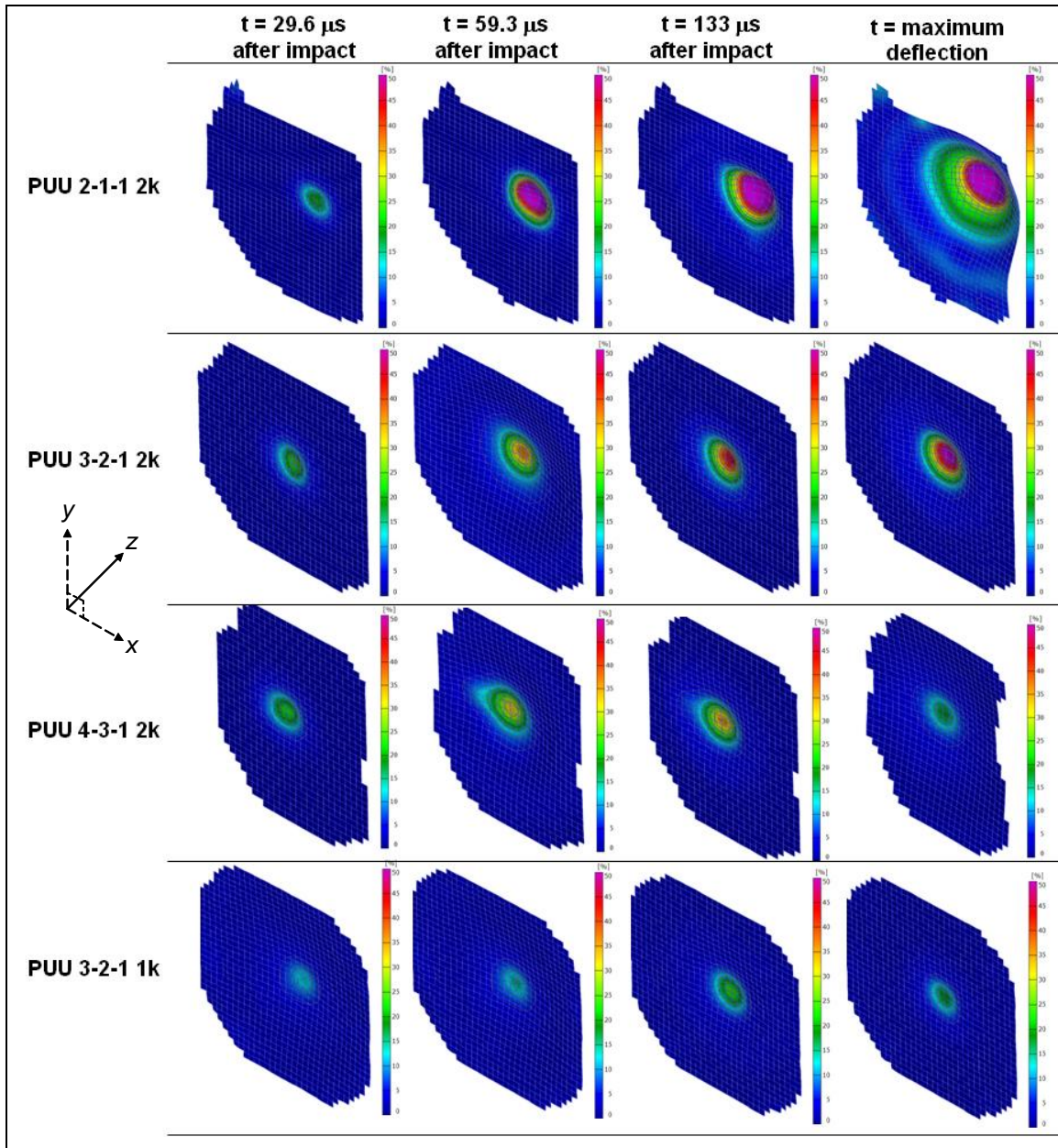
Figure 5. Plots of von Mises deformation strain history measured by impact of PUU 2-1-1 2K, PUU 3-2-1 2K, PUU 4-3-1 2K and PUU 3-2-1 1K against a steel sphere at velocity of 106 m/s.

PUU 2-1-1 2K is the softest elastomer among the select PUU materials. Increasing the hard segment content in the 2K PUU series renders the PUU 4-3-1 2K stiffer; it, therefore, displays more resistance to strain deformation as compared to PUU 3-2-1 2K and PUU 2-1-1 2K. On the other hand, the dynamic strain deformation profile is distinctly different in PUU 3-2-1 1K than the other PUU 2K materials. The PUU 3-2-1 1K is apparently much more resistant to the perforation, and it also shows the most effectiveness in dynamic strain hardening among these four model PUUs. Figure 6 compares the maximum von Mises strain data as a function of time after impact at 106 m/s. The maximum of the von Mises strain refers to the location encountering

the maximum deformation near the vicinity of impact. The PUU 3-2-1 1K reaches the max strain value at the shortest time—about 0.13 ms—compared to 0.18 ms and 0.19 ms observed in PUU 4-3-1 2K and PUU 3-2-1 2K, respectively. Additionally, the max strain value reached in PUU 3-2-1 1K is about 70% of that of PUU 4-3-1 2K and less than 50% of that seen in PUU 3-2-1 2K. The HS content in PUU 3-2-1 1K is nevertheless slightly higher than that of PUU 4-3-1 2K (41% versus 37%). These results indicate that dynamic strain hardening is most significant via altering the SS MW, as seen in PUU 3-2-1 1k, among these PUUs.
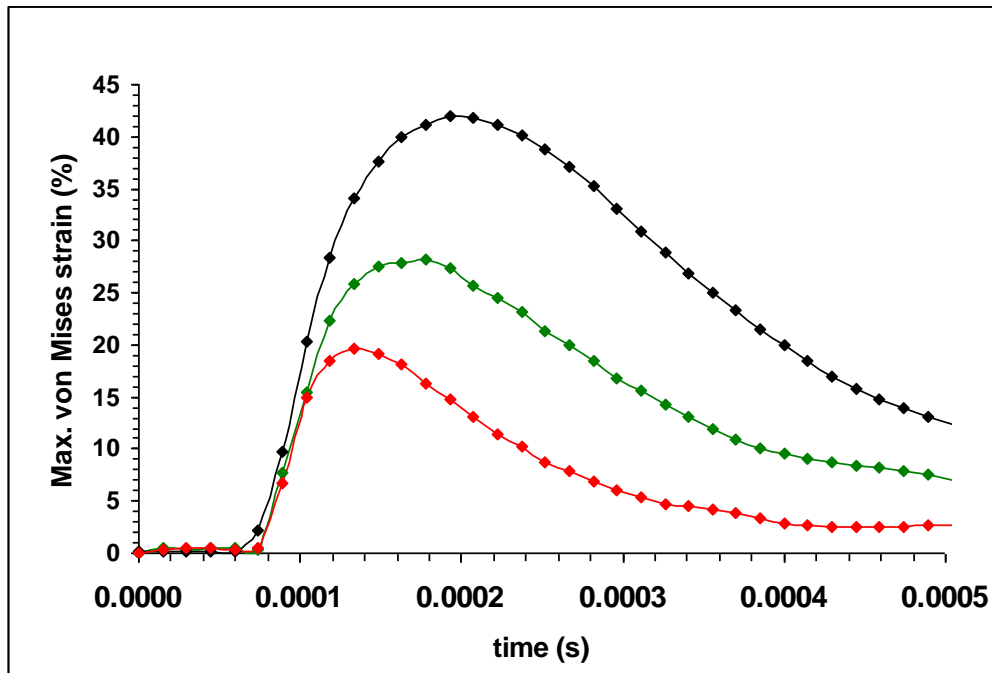

Figure 6. Plots of the maximum von Mises strain as a function of time after impact of PUU 3-2-1 2K (black), PUU 4-3-1 2K (green) and PUU 3-2-1 1K (red).

The effect of impact velocity was also evaluated. Figure 7 is a plot of the von Mises strain evolution of the PUU 2K materials impacted at 142 m/s, which displays similar composition influence on the dynamic strain hardening shown in figure 5.
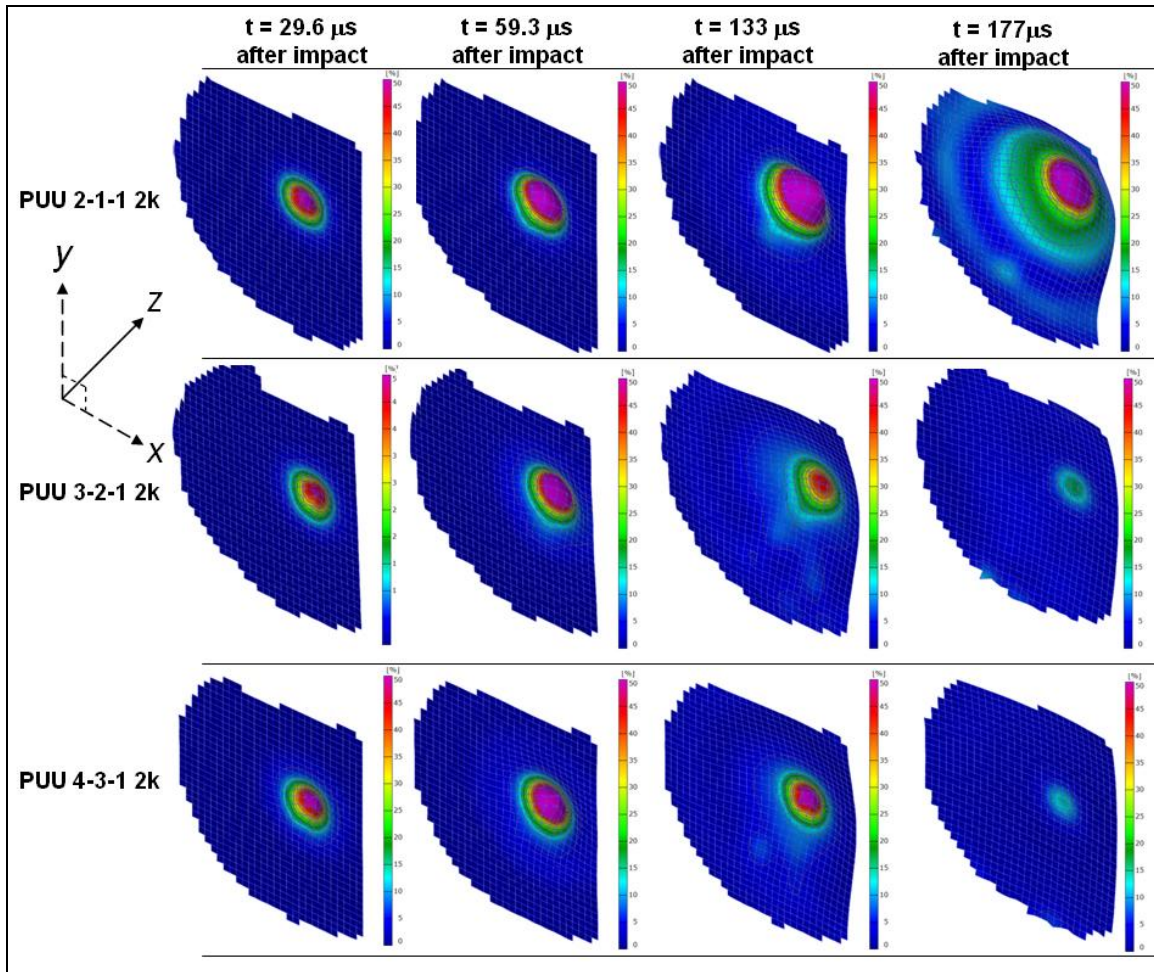
Figure 7. Plots of von Mises deformation strain history measured by impact of PUU 2-1-1 2K, PUU 3-2-1 2K and PUU 4-3-1 2K against a steel sphere at velocity of 142 m/s.

The ARAMIS software also allows for calculation of the shear strain deformation. Figure 8 displays the surface shear strain, ε_{xy}, at times after impact. Based on the evolution of the shear strain propagation data, it clearly shows that PUU 3-2-1 1K exhibits a faster rate in transverse strain wave propagation than PUU 3-2-1 2K, as indicated by faster expanding shear strain contours seen at time 59.3 μs and 133 μs. This suggests that better energy dissipation is associated with the dynamic stiffening in PUU 3-2-1 1K. These measurements also correlate very well with the viscoelastic relaxation data, confirming that the extent of phase mixing, which is composition-dependent, has a significant influence on the high strain-rate deformation in these hyper-elastic PUU materials.
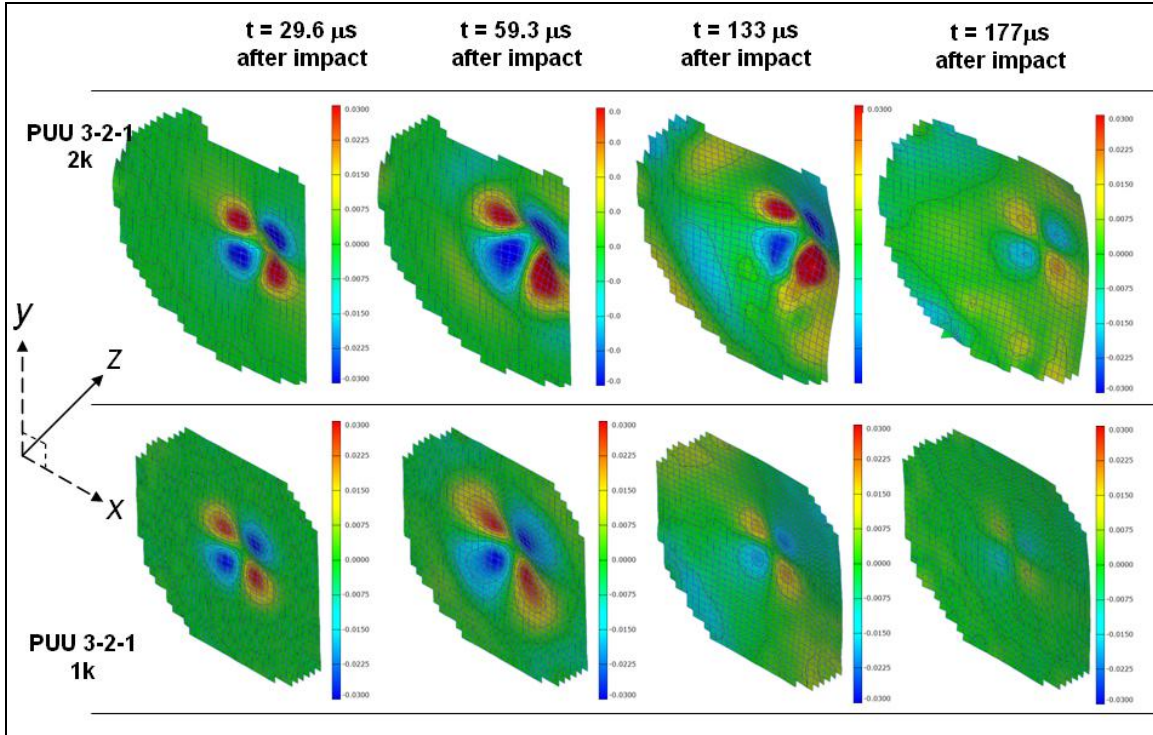
Figure 8. Plots of the surface shear strain, ε_{xy}, of PUU 3-2-1 2K and PUU 3-2-1 1K against a steel sphere at velocity of 142 m/s.

Based on these dynamic impact deformation findings, two additional PUU targets, PUU 2-1-1 650 and PUU 5-4-1 2K, are also included for evaluation. Both these PUU materials have Shore A and Shore D hardness values similar to those of PUU 3-2-1 1K (see Table 1). PUU 2-1-1 650 exhibits a brittle mode of failure (figure 9a), despite the fact that HS% of PUU 2-1-1 650 is 33% much lower than 41% for PUU 3-2-1 1K. This indicates that greater phase mixing promotes dynamic stiffening, yet the choice of SS MW needs to be optimized. PUU 5-4-1 2K has HS content of 44%, and it displays a ductile deformation like the other 2K PUU materials (figure 9b). Further materials characterization of these PUU materials is in progress.
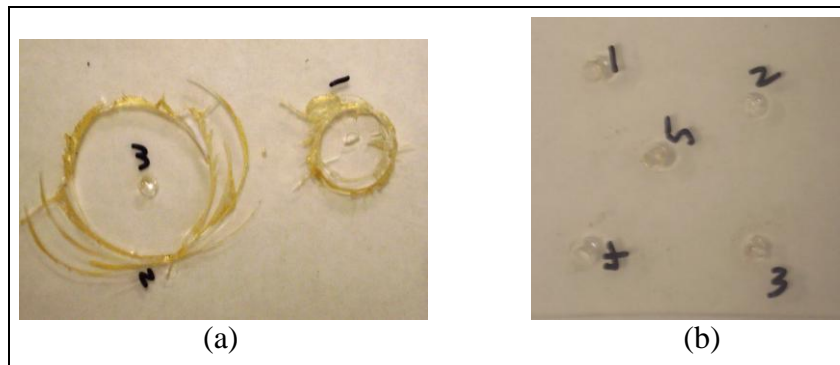

Figure 9. Ballistic impact of (a) PUU 2-1-1 650 and (b) PUU 5-4-1 2K against a 0.22-caliber FSP.

4. Conclusion

A better understanding of molecular influence is invaluable to the design of PUUs for articles that manifest improved protective abilities for Warfighters against the ballistic impact and blast loading hazards. In this work, ballistic impact deformation measurements of select model transparent PUU materials were carried out. The high-speed photogrammetry has demonstrated the capability to reveal and differentiate the composition dependence of the 3D strain deformation histories, which cannot be easily observed quantitatively by other methods. Results indicated that dynamic stiffening by altering the extent of phase mixing appeared to be most important to facilitating the impact stress wave propagation. These high strain-rate mechanical deformation measurements correlated very well with the viscolelastic relaxation data via DMA. Thus, for bulk PUU usage, the choice of SS MW, though critical to phase mixing, requires optimization in addition to maintaining HS% below a threshold value, to ensure a ductile mode of deformation.

5. References

1. Rinaldi, R.; Hsieh A. J.; Boyce M. C. Tunable Microstructures and Mechanical Deformation in Transparent Poly(urethane urea)s (TPUUs), in press. *J. Polym. Sci. Part B. Polym. Phy.* **2010**.

2. Sarva, S.; Hsieh A. J. The Effect of Microstructure on the Rate-dependent Stress-Strain Behavior of Poly(urethane urea) Elastomers. *Polymer* **2009**, *50*, 3007–15.

3. Peters, W. H.; Ranson, W. F.; Sutton, M. A.; Chu, T. C. Applications of Digital Correlation Methods to Rigid Body Mechanics. *Opt. Eng.* **1983**, *22* (6), 738–742.

4. Chu., T. C.; Ranson, W. F.; Sutton, M. A. Applications of Digital-Image-Correlation Techniques to Experimental Mechanics. *Exp. Mech.* **1985**, *25* (3), 232–244.

5. Kahn-Jetter; Chu, T.C. Three-dimensional Displacement Measurements Using Digital Image Correlation and Photogrammic Analysis. *Exp. Mech.* **1990**, *30* (1), 10–16.

6. Gao, Z. B.; Pandya, S.; Hosein, N.; Sacks, M. S.; Hwang, N.H.C. Bioprosthetic Hear Valve Leaflet Motion Monitored by Dual Camera Stereo Photogrammetry. *J. Biomech.* **2000**, *33*, 199–207.

7. Nicolella, D. P.; Nicholls, A. E.; Lankford, J.; Davy, D. T. Machine Vision Photogrammetry: A Technique for Measurement of Microstructural Strain in Cortical Bone. *J. Biomech.* **2001**, *34*, 135–139.

8. Jáuregui, D. V.; White, K. R.; Woodward, C. B.; Leitch K. R. Noncontact Photogrammetric Measurement of Vertical Bridge Deflection. *J. Bridge Eng.* **2003**, *8* (4), 212–222.

9. Kabche, J. P.; Caccese, V.; Berube, K. A.; Thompson, L.; Walls, J. Structural Response of a Hybrid Composite-to-metal Bolted Connection under Uniform Pressure Loading. *Composite Structure* **2007**, *78*, 207–221.

10. Melis, M. E.; Brand, J. B.; Pereira, J. M.; Revilock, D. M. *Reinforce Carbon-carbon Subcomponent Flat Plate Impact Testing for Space Shuttle Orbiter Return to Flight*; NASA Report NSAS/TM-2007-214384; 2007.

11. Tiwari,V.; Sutton, M. A.; McNeil, S. R.; Xu, S.; Deng, X.; Fourney, W.; Bretall, D. Application of 3D Image Correlation for Full-field Transient Plate Deformation Measurements during Blast Loading. *Int'l J. Impact Eng.* **2009**, *36*, 862–874.

12. Yu, J. H.; Hsieh A. J.; Dehmer, P. G.; Sands, J. M. Real-time Full-field Deformation Analysis on the Ballistic Impact of Polymeric Materials Using High-speed Photogrammetry. *Proceedings, American Society for Composites 2009 − 24th Technical Conference*, University of Delaware, Newark, DE, 15-17 September 2009.

13. Yu, J. H.; Dehmer, P. G. *Dynamic Impact Deformation Analysis Using High speed Cameras and ARAMIS Photogrammetry Software*; ARL-TR-5212; U.S. Army Research Laboratory: Aberdeen Proving Ground, MD, June 2010.

14. O'Sickey, M. J.; Lawrey, B. D.; Wilkes, G. L. Structure-property Relationships of Poly(urethane urea)s with Ultra-low Monol Content Poly(propylene glycol) Soft Segments. I. Influence of Soft Segment Molecular Weight and Hard Segment Content. *Polymer* **2002**, *43*, 7399–7408.

15. ASTM D2240, 2010. Standard Test Method for Rubbery Property − Durometer Hardness.

16. Kojio K.; Nakashima S.; Furukawa M. Microphase-separated Structure and Mechanical Properties of Norbornane Diisocyanate-based Polyurethanes. *Polymer* **2007**, *48*, 997–1004.

17. Schmidet, T.; et al. Full-field dynamic displacement and strain measurement using advanced 3D image correlation photogrammetry: Pat 1. Experimetal Techniques, pp 47–50, 2003.

18. Tiwari, V.; et al. Application of 3D Image Correlation for Full-field Transient Plate Deformation Measurements During Blast Loading. *International Journal of Impact Engineering* **2009**, 36, 862–874

No. of
Copies   Organization

   1   ADMNSTR
 ELEC   DEFNS TECHL INFO CTR
         ATTN DTIC OCP
         8725 JOHN J KINGMAN RD STE 0944
         FT BELVOIR VA 22060-6218

   3   US ARMY RSRCH LAB
         ATTN IMNE ALC HRR
         MAIL & RECORDS MGMT
         ATTN RDRL CIM L TECHL LIB
         ATTN RDRL CIM P TECHL PUB
         ADELPHI MD 20783-1197

   1   US ARMY RSRCH LAB
         ATTN RDRL CIM G T LANDFRIED
         BLDG 4600
         ABERDEEN PROVING GROUND MD
         21005-5066

 7 HCS   US ARMY RSRCH LAB
         ATTN RDRL-WMM-B
          B. CHEESEMAN
          M. VANLANDINGHAM
          J YU
         ATTN RDRL-WMM-D
          S WALSH
         ATTN RDRL-WMM-G
         A.   RAWLETT
         J. LENHART
         A. HSIEH

INTENTIONALLY LEFT BLANK.